Journal of Exploratory Research in Pharmacology **2021** vol. 6(3) | 71–86
DOI: 10.14218/JERP.2021.00011

Original Article

Network Pharmacology Elucidates the Anti-Inflammatory Mechanisms of QingFeiPaiDu Decoction for Treatment of COVID-19

Yan Liu[#], Lewen Xiong[#], Yanyu Wang, Mengxiong Luo, Longfei Zhang[*] and Yongqing Zhang[*]

School of Pharmacy, Shandong University of Traditional Chinese Medicine, Jinan, China

Received: May 08, 2021 | **Revised:** June 30, 2021 | **Accepted:** July 9, 2021 | **Published:** July 30, 2021

Abstract

Background and objectives: QingFeiPaiDu decoction (QFPDD) treatment benefits patients with coronavirus disease 2019 (COVID-19). This study aims to elucidate the mechanisms that underlie the anti-inflammatory effects of QFPDD.

Methods: Based on the clinical symptoms of COVID-19 patients, a component-target-disease network was constructed using the network pharmacology method, and the potential active components, targets, and molecular mechanisms of QFPDD for the treatment of COVID-19 were screened using topology parameter analysis. The best molecules that were affected by QFPDD were validated using Real-Time quantitative polymerase chain reaction (RT-qPCR) in a cellular inflammation model.

Results: In total, 376 active ingredients were identified in QFPDD, and 18,833 potential anti-severe acute respiratory syndrome coronavirus 2 (SARS-CoV-2) targets. The principal targets included *PIK3CA*, *PIK3R1*, *APP*, *SRC*, *MAPK1*, *MAPK3*, *AKT1*, *HSP90AA1*, *EP300*, and *CDK1*. Overall, 574 gene oncology entries and 214 signal pathways were identified. QFPDD affected the cellular response to nitrogen compounds, protein kinase activity, and membrane rafts. QFPDD modulated pathways that are associated with cancer, endocrine resistance, PI3K-Akt signaling, and proteoglycans in cancer. Molecular docking indicated that the core ingredients of QFPDD had a strong binding affinity for SARS-CoV-2 3-chymotrypsin-like cysteine protease (3CLpro) and angiotensin-converting enzyme 2 (ACE2). QFPDD treatment significantly mitigated the lipopolysaccharides-induced five targeted gene transcription in A549 cells.

Conclusions: Our findings preliminarily elucidated that through its active ingredients QFPDD targeted 3CLpro and ACE2 to modulate many factors and pathways that are associated with the pathogenesis of COVID-19. The identified potential molecular mechanism, relevant factors, and key genes QFPDD targeted might help in the design of new and specific antiviral drugs.

Keywords: QingFeiPaiDu decoction; COVID-19; Bioactive ingredients; Molecular mechanism; Network pharmacology; Cell experiment.

Abbreviations: 3CLpro, 3-chymotrypsin-like cysteine protease; ACE2, angiotensin-converting enzyme; AFI, Aurantii Fructus Immaturus; ALI, acute lung injury; AMR, Atractylodis Macrocephalae Rhizoma; AR, Alismatis Rhizoma; ARR, Asari Radix et Rhizoma; ASA, Armeniacae by Amarum; ASPL, average shortest path length; AST, Asteris Radix et Rhizoma; BC, betweenness centrality; BR, Belamcandae Rhizoma; BUP, Bupleuri Radix; CC, closeness centrality; COVID-19, coronavirus disease 2019; CR, Cinnamomi Ramulus; CRP, Citri Reticulatae Pericarpium; DR, Dioscoreae Rhizoma; EH, Ephedrae Herba; FF, Farfarae Flos; G, FGypsum Fibrosum; GRR, Glycyrrhizae Radix et Rhizoma; MAPK1, mitogen-activated protein kinase 1; PH, Pogostemonis Herba; POL, Polyporus; POR, Poria; PR, Pinelliae Rhizoma; PRKCD, protein kinase C delta; PRKCE, protein kinase C epsilon.; PTK2, protein tyrosine kinase 2; QFPDD, QingFeiPaiDu Decoction; SR, Scutellariae Radix; SRC, SRC proto-oncogene, non-receptor tyrosine kinase; TCM, traditional Chinese medicine; ZRR, Zingiberis Rhizoma Recens.

[*]**Correspondence to**: Longfei Zhang and Yongqing Zhang, School of Pharmacy, Shandong University of Traditional Chinese Medicine, Jinan 250355, China. ORCID: https://orcid.org/0000-0003-1894-4504 (LFZ), https://orcid.org/0000-0002-2711-6770 (YQZ). Tel: +86 0531-89628192 (LFZ), +86 0531-89628080 (YQZ), Fax: +86 0531-89628192 (LFZ), +86 0531-89628080 (YQZ), E-mail: longfei_zhang@sdutcm.edu.cn (LFZ), zyq622003@126.com (YQZ)

[#]Both authors contributed equally to this work.

How to cite this article: Liu Y, Xiong L, Wang Y, Luo M, Zhang L, Zhang Y. Network Pharmacology Elucidates the Anti-Inflammatory Mechanisms of QingFeiPaiDu Decoction for Treatment of COVID-19. *J Explor Res Pharmacol* 2021;6(3):71–86. doi: 10.14218/JERP.2021.00011.

Introduction

The coronavirus 2019 (COVID-19) pandemic was caused by a severe acute respiratory syndrome coronavirus 2 (SARS-CoV-2) infection.[1] To date, although several vaccines have been used for the prevention of COVID-19, novel coronavirus variants have spread worldwide. In March 2021, the Delta SARS-CoV-2 variant was identified in India and has now spread to >100 countries. However, there is no clinically effective therapy against the SARS-CoV-2 infection. Of note, traditional Chinese medicine (TCM) has unique advantages in anti-inflammation and control of infectious diseases. The QingFeiPaiDu decoction (QFPDD) is composed of four classic prescriptions of ephedra, apricot kernel, gypsum, and licorice decoction, the Belamcanda and ephedra decoction, the Minor Bupleurum Decoction, and the Powder of Five Ingredients with Poria. A previous study showed that treatment with QFPDD effectively relieved fever, cough, fatigue, and other symptoms in newly diagnosed COVID-19 patients and rapid cleans SARS-CoV-2 to prevent severe disease as well as reduces the mortality rate of hospitalized severe COVID-19 patients.[2] Currently, QFPDD has been approved for the treatment of COVID-19 patients by the Chinese government. Therefore, it is of great significance to explore the mechanisms that underlie the action of QFPDD in the treatment of COVID-19.

QFPDD contains 21 TCMs with complicated ingredients, and the clinical efficacy of QFPDD could result from combinational effects of its multi-ingredients that target several molecules and pathways as well as systemic body regulation. To develop new anti-SARS-CoV-2 drugs, a network pharmacological analysis[3] was used to explore the active ingredients and potential molecular mechanisms that underlie the anti-inflammatory activity of QFPDD for the treatment of COVID-19, based on the main clinical symptoms of COVID-19 patients. The research workflow is shown in Figure 1.

Materials and methods

Collection of the active ingredients of QFPDD

Using the Traditional Chinese Medicine Systems Pharmacology (www.tcmspw.com/index.php) and Traditional Chinese Medicines Integrated Database (www.119.3.41.228:8000/tcmid/search), the potential active ingredients of QFPDD were screened, according to the criteria of oral bioavailability (OB) ≥30% and a drug-likeness (DL) ≥0.18. Gypsum fibrosum is a mineral medicine with a relatively simple composition. Gypsum fibrosum was included in the study although it did not meet the criteria.

Prediction of the targets of active ingredients of QFPDD

Using the PubChem database (www.pubchem.ncbi.nlm.nih.gov) and the SwissTargetPrediction database (www.swisstargetprediction.ch), the potential targets for the active ingredients of QFPDD were predicted (eliminated if $p = 0$ and the target was screened if p>median).

Screening of the main active ingredients and targets of QFPDD

The main active ingredients and targets for QFPDD were screened, according to the average degree of freedom and the maximum degree of freedom. The ingredient–target network diagram was constructed using Cytoscape software (version 3.7.2), and the network topology parameters were calculated using the Cytoscape tools.

Identification of the targets of the major COVID-19 clinical symptoms

The main symptoms of mild COVID-19 patients included fever, cough, and fatigue. The corresponding disease targets were screened using the GeneCards database (www.genecards.org), TTD database (www.db.idrblab.net/ttd), DrugBank database (www.drugbank.ca), DisGeNet database (www.disgenet.org/search) and OMIM database (www.omim.org).

Construction and analysis of the QFPDD-COVID-19-Target network

The main active ingredient targets and disease targets were established as pairs to obtain the potential targets for QFPDD in the treatment of COVID-19. The obtained data were used to construct the QFPDD-COVID-19-Target network using Cytoscape software (version 3.7.2). The topological parameters of the constructed network were analyzed to explore the interaction between different TCMs in QFPDD for the treatment of COVID-19.

Construction and analysis of potential protein–protein interactions

The potential targets of QFPDD in the treatment of COVID-19 were imported into the STRING database (www.string-db.org), and the protein–protein interaction (PPI) network of potential targets was obtained, based on a confidence score of ≥0.9 for the interaction targets. Then, the topology parameters that included each node degree, the betweenness centrality (BC), closeness centrality (CC), average shortest path length (ASPL), and the average values of the potential targets for QFPDD were analyzed using Cytoscape software (version 3.7.2).

Gene Ontology enrichment analysis and Kyoko Encyclopedia of Genes and Genomes pathway analysis

The potential targets of QFPDD for the treatment of COVID-19 were analyzed by Gene Ontology (GO) enrichment analysis, and the potential human signal pathways of the targets involved were analyzed using the DAVID website (www.david.ncifcrf.gov) and Kyoko Encyclopedia of Genes and Genomes (KEGG) database with a p-value of 0.05.

Molecular docking

The three-dimensional (3D) structures of the SARS-CoV-2 3-chymotrypsin-like cysteine protease (3CLpro) (PDB ID: 6LU7) and angiotensin-converting enzyme 2 (ACE2) (PDB ID: 1R42) were downloaded from the RCSB database (www.rcsb.org). The original receptor proteins were extracted, and water molecules, other ligands, and residues were removed using PyMOL 1.7.2.1 software. AutoDock Tools 1.5.6 software was used for hydrogenation, merging of nonpolar and hydrogen interactions, and conversion into PDBQT format. The two-dimensional (2D) or 3D structures of the ligand compounds were downloaded from the PubChem

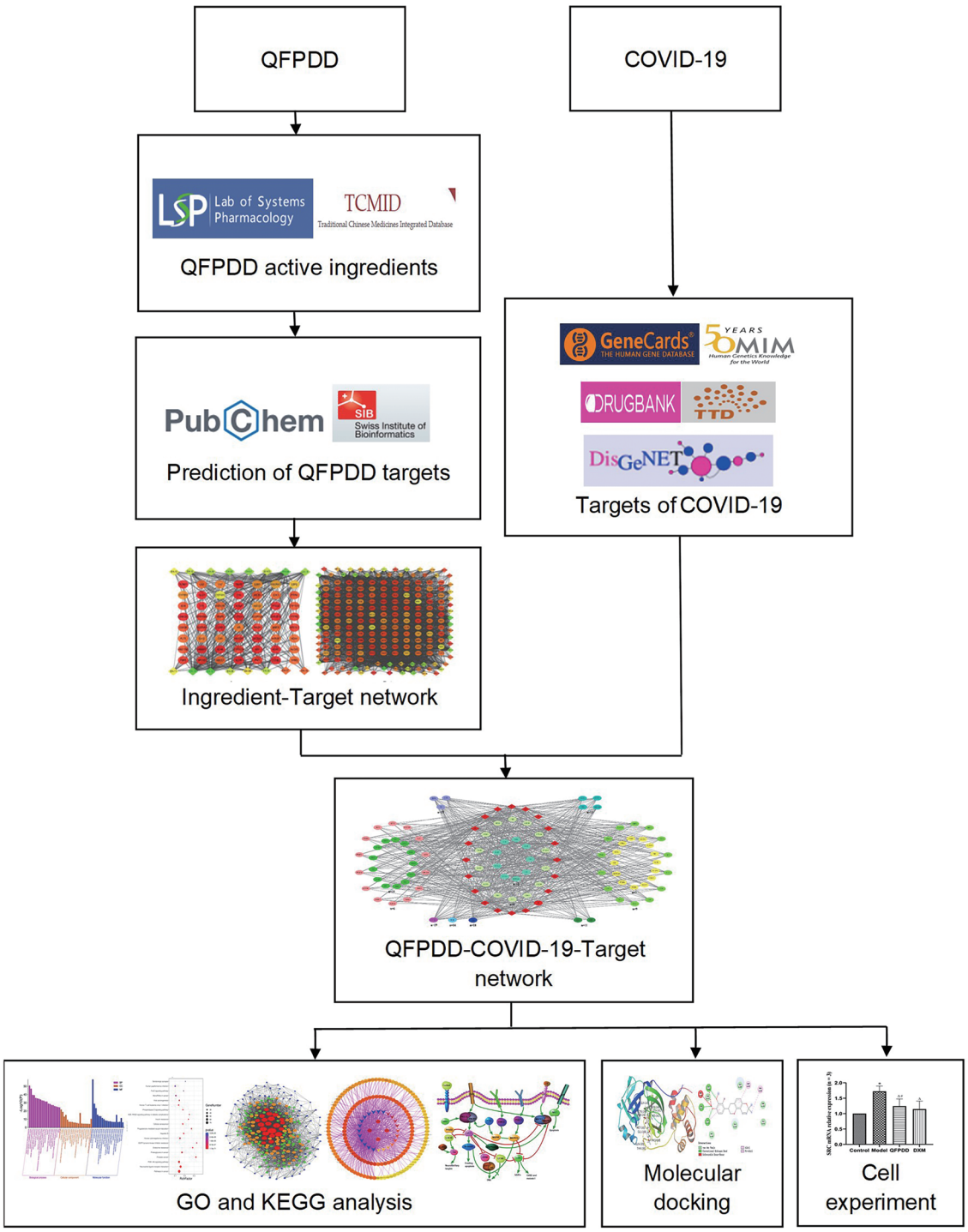

Fig. 1. Illustration of the workflow when studying QFPDD in the treatment of COVID-19.

database. The energy of the ligand compounds was minimized and saved in mol2 format with ChemBioOffice 2016 software. All of the flexible bonds of the ligand compounds were rotated by default. The grid box that was used for molecular docking included all the surrounding residues and centered on the primary ligands of the receptor proteins. The molecular docking was performed using Autodock Vina 1.1.2 and a Python script, and the sequences were sorted, according to the optimal affinity of each ligand compound.

Real-Time qPCR verifies the effect of QFPDD on gene expression

Gypsum fibrosum was decocted first, and all the TCMs were de-

Table 1. Sequences of primers for RT-qPCR

Target gene	Forward sequence and reverse sequence	Product length (bp)
β-actin	F: TGACGTGGACATCCGCAAAG	204
	R: CTGGAAGGTGGACAGCGAGG	
SRC	F: GCTTCAACTCCTCGGACACC	168
	R: ACCAGTCTCCCTCTGTGTTGTT	
MAPK1	F: CCAGGGAAGCATTATCTTGACC	172
	R: CTTTGGAGTCAGCATTTGGGAA	
PRKCD	F: AGCACAGAGCGTGGGAAAAC	146
	R: GTCACCTCAGACACTGGCTCCT	
PTK2	F: ATCTATCCAGGTCAGGCATCTCT	179
	R: ATTTCCTGTTGCTGTCGGATTAG	
PRKCE	F: ATGCCCCCATAGGCTACGAC	153
	R: CACCCGACGACCCTGAGAG	

SRC, SRC proto-oncogene, non-receptor tyrosine kinase; MAPK1, mitogen-activated protein kinase 1; PRKCD, protein kinase C delta; PTK2, protein tyrosine kinase 2; PRKCE, protein kinase C epsilon.

cocted twice with 1:8 (weight/weight) of water. The TCM liquid was concentrated to 76 mL, freeze-dried and ground into a fine powder with liquid nitrogen.

Human lung cancer A549 cells were obtained from the Chinese Academy of Sciences Stem Cell Bank. The cells (1×10^5 cells/well) were stimulated with 10 μg/mL lipopolysaccharides (LPS; L8880, Solarbio, Beijing, China) alone or LPS combined with 6.4 mg/mL QFPDD or 0.02 μmol/L Dexamethasone (DXM), for 24 h. The cells were harvested, and their total RNA was extracted, followed by reverse transcription into cDNA using a reverse transcription kit (RR047A, Takara, Beijing, China). The relative levels of the target to the control β-actin mRNA transcripts were quantified by Real-Time quantitative polymerase chain reaction (RT-qPCR) using specific primers (Table 1). The data were analyzed by $2^{-\Delta\Delta CT}$.

Statistical analysis

All data are expressed as mean ± standard deviation. Analysis of variance (ANOVA) was used to evaluate the statistical difference in data that met normal distribution and homogeneity of variance. A rank sum test was used when data did not meet a normal distribution or heterogeneity of variance. $p>0.05$ indicated no statistical difference. $p<0.05$ indicated statistical difference. $p<0.01$ indicated a significant difference.

Results

Active ingredients of QFPDD

There were 376 ingredients with an OB ≥30% and a DL ≥0.18 in the 20 TCMs and gypsum fibrosum: Ephedrae Herba (EH) contained 23, Glycyrrhizae Radix et Rhizoma (GRR) 92, Armeniacae by Amarum (ASA) 19, Gypsum Fibrosum (GF) 1, Cinnamomi Ramulus (CR) 7, Alismatis Rhizoma (AR) 10, Polyporus (POL) 11, Atractylodis Macrocephalae Rhizoma (AMR) 7, Poria (POR) 15, Bupleuri Radix (BUP) 17, Scutellariae Radix (SR) 36, Pinelliae Rhizoma (PR) 13, Zingiberis Rhizoma Recens (ZRR) 5, Asteris Radix et Rhizoma (AST) 19, Farfarae Flos (FF) 22, Belamcandae Rhizoma (BR) 17, Asari Radix et Rhizoma (ARR) 8, Dioscoreae Rhizoma (DR) 16, Aurantii Fructus Immaturus (AFI) 22, Citri Reticulatae Pericarpium (CRP) 5, and Pogostemonis Herba (PH) with 11 ingredients (Supplementary Document 1, sheet 1). Because Asteris Radix et Rhizoma and Asari Radix et Rhizoma have the same Latin initials, to distinguish between both TCMs, the first three letters of the first word of Asteris Radix et Rhizoma were used to represent this TCM.

The potential targets of active ingredients in QFPDD

A total of 18,833 targets were predicted by the 376 active ingredients in QFPDD (except for the targets of GF and some active ingredients that had not been identified). The detailed information on the targets of 20 TCMs' active ingredients in QFPDD is shown in Supplementary Document 2.

Main active ingredients of QFPDD and their potential targets

Many ingredients of QFPDD might be helpful in the treatment of COVID-19; however, the main ingredients of QFPDD were used to elucidate the mechanism that underlies its pharmacological action. An ingredient–target network was constructed (Fig. 2) using these 20 TCMs and their abbreviations in Supplementary Document 1 (sheet 2). According to the ingredient–target network, there were 39 core ingredients and their corresponding targets (Table 2).

Targets are associated with clinical symptoms of COVID-19

To explore the molecular mechanism that underlies the action of QFPDD, 9,624 targets that were associated with common COVID-19 clinical symptoms, such as fever, cough, and fatigue were screened from the database (Supplementary Document 1, sheet 3).

QFPDD-COVID-19-Target network

Different TCMs might act synergistically on the same target when treating COVID-19 and enhance the therapeutic efficacy. A network of TCMs and the targets of ≥6 TCMs was generated in Figure 3. Among these targets, 19 TCMs targeted CYP19A1, and 18 targeted ESR2; 15 TCMs shared 3 common targets, and 14 targeted SHBG. In addition, 13 TCMS mutually targeted 4 targets, 12 TCMs shared 9 targets, 11 TCMs targeted 2 targets, 10 TCMs shared13 targets, 9 TCMs had the same 14 targets, 8 TCMs had 14 targets, 7 TCMs had 14 targets, and 6 TCMs shared14 targets. Therefore, TCMs had a multi-ingredient-multitarget feature for the treatment of COVID-19.

PPI network

The potential targets of QFPDD for the treatment of COVID-19 were analyzed using the STRING database, and the PPI network of protein interactions was obtained. Through the calculation of the degree of each node, the BC, CC, and the ASPL, 24 key targets

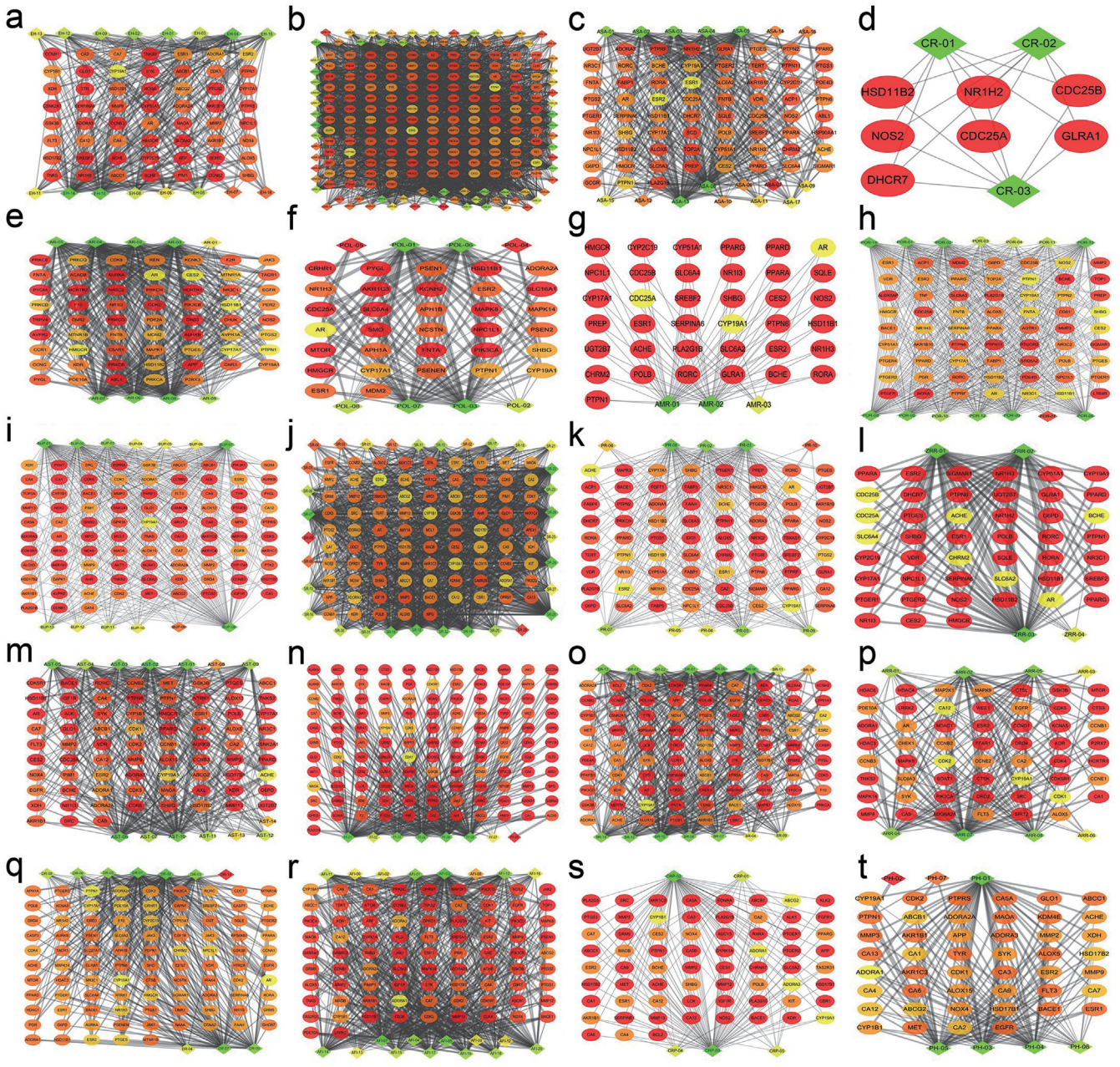

Fig. 2. Ingredient–target network: (a) EH; (b) GRR; (c) ASA; (d) CR; (e) AR; (f) POL; (g) AMR; (h) POR; (i) BUP; (j) SR; (k) PR; (l) ZRR; (m) AST; (n) FF; (o) BR; (p) ARR; (q) DR; (r) AF; (s) CRP; and (t) PH. The rhomboid node represents the ingredient, and the circular node represents the target. The color of the node represents the degrees of freedom in ascending order from red to yellow to green, and the size of the edge betweenness is denoted by the thickness of the line.

were selected (Table 3).

GO enrichment analysis and KEGG pathway analysis

The GO enrichment analysis of the potential targets of QFPDD for the treatment of COVID-19 revealed 574 GO entries with $p<0.05$, a minimum count of 3 and an enrichment factor >1.5 (the enrichment factor is the ratio between the observed number and the number expected by chance), which included 353 entries for biological processes, 112 for molecular function, and 109 for cell composition. The top enriched 20 biological process entries in each category are shown in Figure 4a. The KEGG pathway analysis indicated that 214 signal pathways were involved. They included the PI3K-Akt, JAK-STAT, AMPK, NOD-like receptor, NF-κB, Notch, TGF-β, and HIF-1 signal pathways[4–15] that are associated with the pathogenesis of pneumonia. The top 20 signal pathways are shown in Figure 4b. There were 196 signal pathways with a $p<0.01$, and 262 genes were associated with these pathways. Their correlation was established in Figure 5. The 24 critical targets that were identified by network analysis had high degree values. These genes might be the critical target genes of

Table 2. Main or core active ingredients and their targets in 20 TCMs

Chinese name	Latin name	Number of main ingredients	Core ingredients	Core targets
麻黄	Ephedrae Herba	16	diosmetin (EH-10); genkwanin (EH-14); kaempferol (EH-04)	*CYP19A1*
炙甘草	Glycyrrhizae Radix et Rhizoma	75	3'-Methoxyglabridin (GRR-63); glypallichalcone (GRR-26); glyasperin B (GRR-18)	*CYP19A1; PTPN1; ESR2; ESR1*
杏仁	Armeniacae Semen Amarum	17	gondoic acid (ASA-13); spinasterol (ASA-08)	*ESR1; ESR2*
桂枝	Cinnamomi Ramulus	3	peroxyergosterol (CR-03); sitosterol (CR-02); beta-sitosterol (CR-01)	*HSD11B2; CDC25A; NOS2; NR1H2; GLRA1; DHCR7; CDC25B*
泽泻	Alismatis Rhizoma	9	alisol,b,23-acetate (AR-04); [(1S,3R)-1-[(2R)-3,3-dimethyloxiran-2-yl]-3-[(5R,8S,9S,10S,11S,14R)-11-hydroxy-4,4,8,10,14-pentamethyl-3-oxo-1,2,5,6,7,9,11,12,15,16-decahydrocyclopenta[a]phenanthren-17-yl]butyl] acetate (AR-08); alisol B monoacetate (AR-03)	*AR; CES2; CYP17A1; HMGCR; HSD11B1; PTPN1*
猪苓	Polyporus	8	(22e,24r)-ergosta-6-en-3beta,5alpha,6beta-triol (POL-03); Cerevisterol (POL-01)	*AR*
白术	Atractylodis Macrocephalae Rhizoma	3	α-Amyrin (AMR-01); (3S,8S,9S,10R,13R,14S,17R)-10,13-dimethyl-17-[(2R,5S)-5-propan-2-yloctan-2-yl]-2,3,4,7,8,9,11,12,14,15,16,17-dodecahydro-1H-cyclopenta[a]phenanthren-3-ol (AMR-02)	*CYP19A1; AR; CDC25A*
茯苓	Poria	14	3beta-Hydroxy-24-methylene-8-lanostene-21-oic acid (POR-09); trametenolic acid (POR-02); dehydroburicoic acid (POR-14)	*SHBG; PTPN1; HSD11B1*
柴胡	Bupleuri Radix	13	3,5,6,7-tetramethoxy-2-(3,4,5-trimethoxyphenyl)chromone(BUP-07); quercetin (BUP-01); areapillin (BUP-08)	*CYP19A1*
黄芩	Scutellariae Radix	32	5,8,2'-Trihydroxy-7-methoxyflavone (SR-13); moslosooflavone (SR-28)	*ESR2*
姜半夏	Pinelliae Rhizoma	10	beta-sitosterol (PR-01); gondoic acid (PR-08)	*ACHE; CYP19A1; ESR2*
生姜	Zingiberis Rhizoma Recens	4	beta-sitosterol (ZRR-01); poriferast-5-en-3beta-ol (ZRR-03); stigmasterol (ZRR-02)	*AR; ACHE; SLC6A2; BCHE; SLC6A4; CHRM2; CDC25A; CDC25B*
紫菀	Asteris Radix et Rhizoma	14	quercetin (AST-02); galangin (AST-06)	*ACHE; CYP19A1*
冬花	Farfarae Flos	8	quercetin (FF-01); femara (FF-08); tussilagolactone (FF-06)	*CDK1*
射干	Belamcandae Rhizoma	15	epianhydrobelachinal (BR-10); anhydrobelachinal (BR-06)	*CYP19A1; CA2*
细辛	Asari Radix et Rhizoma	8	4,9-dimethoxy-1-vinyl-$b-carboline (ARR-07)	*CDK1; CDK2; CYP19A1; CA12*
山药	Dioscoreae Rhizoma	10	denudatin B (DR-01); kadsurenone (DR-02)	*CYP19A1; PTPN1; AR*
枳实	Aurantii Fructus Immaturus	20	sinensetin (AFI-03)	*ADORA1*
陈皮	Citri Reticulatae Pericarpium	5	5,7-dihydroxy-2-(3-hydroxy-4-methoxyphenyl) chroman-4-one (CRP-03); naringenin (CRP-02)	*ABCG2; ADORA1; ADORA3; CYP19A1; CYP1B1*
藿香	Pogostemonis Herba	7	quercetin (PH-01)	*ADORA1*

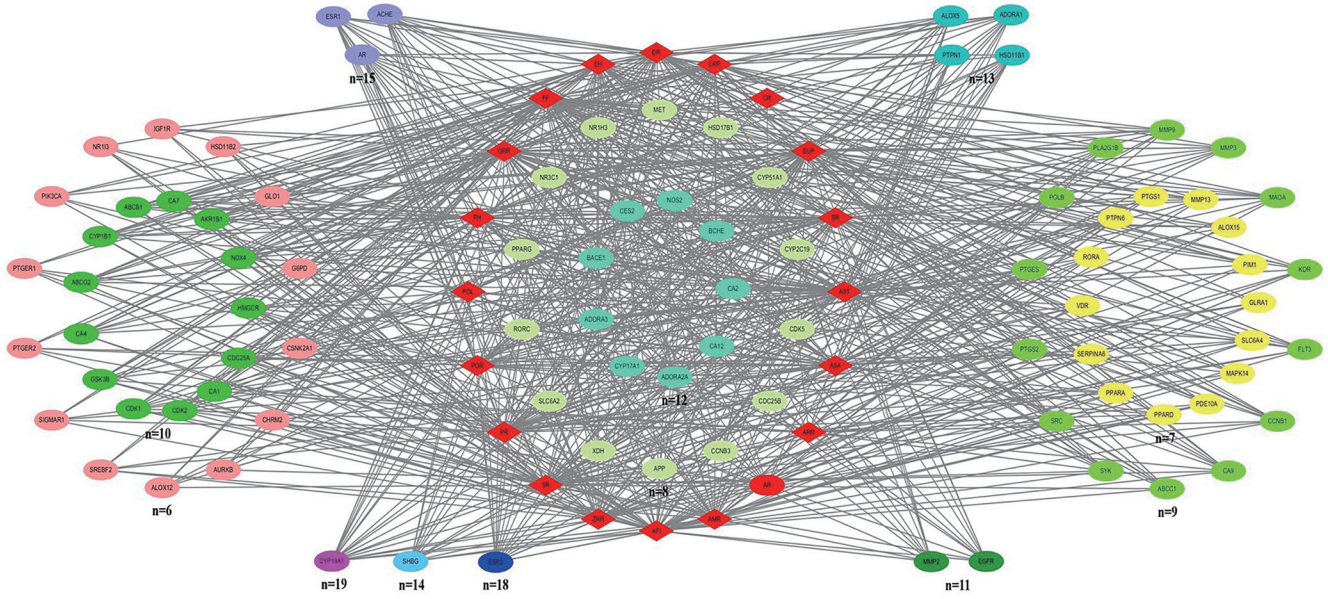

Fig. 3. QFPDD-COVID-19 Target Network. Rhomboid node represents TCMs, the circular node the target, and n = number of types of targets in the same circle to the same amount of TCMs.

Table 3. Topological analysis of the QFPDD-COVID-19 Target network

Target name	Abbreviation	Uniprot ID	ASPL	BC	CC	Degree
Phosphatidylinositol-4,5-bisphosphate 3-kinase catalytic subunit alpha	*PIK3CA*	P42336	2.189	0.098	0.457	66
Phosphoinositide-3-kinase regulatory subunit 1	*PIK3R1*	P27986	2.205	0.086	0.454	62
Amyloid beta precursor protein	*APP*	P05067	2.358	0.166	0.424	55
SRC proto-oncogene, non-receptor tyrosine kinase	*SRC*	P12931	2.280	0.053	0.439	49
mitogen-activated protein kinase 1	*MAPK1*	P28482	2.130	0.084	0.470	47
mitogen-activated protein kinase 3	*MAPK3*	P27361	2.224	0.042	0.450	43
AKT serine/threonine kinase 1	*AKT1*	P31749	2.268	0.063	0.441	40
heat shock protein 90 alpha family class A member 1	*HSP90AA1*	P07900	2.311	0.065	0.433	38
E1A binding protein p300	*EP300*	Q09472	2.453	0.065	0.408	34
cyclin dependent kinase 1	*CDK1*	P06493	2.614	0.033	0.382	30
Janus kinase 2	*JAK2*	O60674	2.512	0.017	0.398	30
epidermal growth factor receptor	*EGFR*	P00533	2.370	0.041	0.422	29
Thrombin	*F2*	P00734	2.508	0.033	0.399	28
mitogen-activated protein kinase 8	*MAPK8*	P45983	2.283	0.045	0.438	28
retinoid X receptor alpha	*RXRA*	P19793	2.500	0.072	0.400	27
estrogen receptor 1	*ESR1*	P03372	2.382	0.090	0.420	27
protein kinase C delta	*PRKCD*	Q05655	2.563	0.015	0.390	23
protein tyrosine kinase 2	*PTK2*	Q05397	2.618	0.012	0.382	22
ribosomal protein S6 kinase B1	*RPS6KB1*	P23443	2.480	0.012	0.403	21
mitogen-activated protein kinase 14	*MAPK14*	Q16539	2.567	0.012	0.390	21
nuclear receptor subfamily 3 group C member 1	*NR3C1*	P04150	2.430	0.022	0.412	21
protein kinase C epsilon	*PRKCE*	Q02156	2.594	0.015	0.385	17
cyclin dependent kinase 5	*CDK5*	Q00535	2.634	0.028	0.380	17
peroxisome proliferator activated receptor alpha	*PPARA*	Q07869	2.587	0.031	0.387	15

ASPL, average shortest path length; BC, betweenness centrality; CC, closeness centrality.

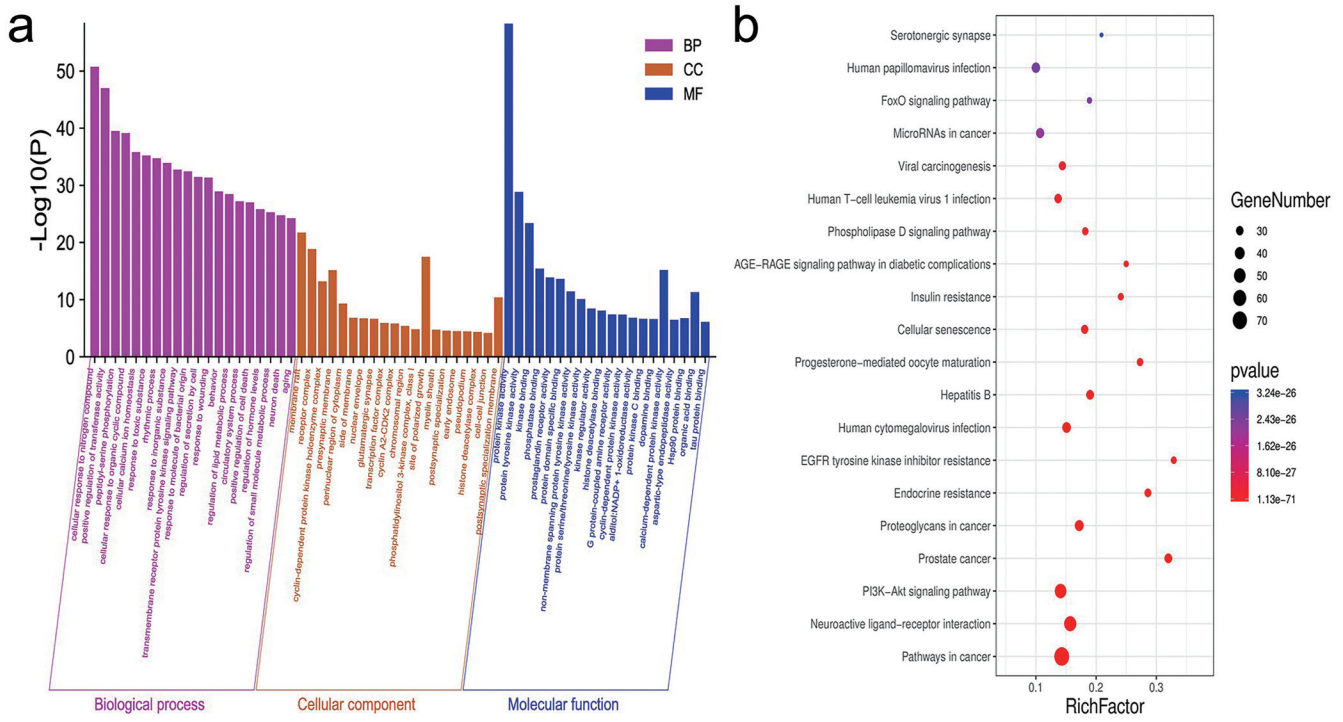

Fig. 4. GO enrichment and KEGG pathway analyses for the potential targets of QFPDD: (a) enrichment analysis of biological processes, molecular functions and cell ingredients; and (b) KEGG pathway analysis. The size of the bubble represents the gene count for this line, and the color from blue to red represents the *p*-values from large to small.

QFPDD for the treatment of COVID-19. According to the statistics on the occurrence of the 24 critical targets in 196 signaling pathways, 24 targets were involved in 156 signal pathways (Fig. 6), which included pathways involved in cancer, endocrine resistance, the PI3K-Akt signal pathway, proteoglycans in cancer, and the Rap1 signal pathway. The Rap1 signaling pathway is crucial for the pathogenesis of acute lung injury or acute respiratory distress syndrome (ALI/ARDS), and the regulation of the Rap1 signaling pathway might become a new strategy for the treatment of ALI/ARDS.[16] A diagram of the 24 critical targets for the treatment of COVID-19 is shown in Figure 7.

Molecular docking results

In total, 375 active ingredients from 20 TCMs (except for GF) in QFPDD were selected and screened for their binding to ACE2 and 2019-nCoV 3CLpro by molecular docking, based on the binding energy. The lower the binding energy, the higher the possibility of binding. The docking results indicated that the binding energies of the 375 main active ingredients were all <0 (except for taraxanthin and delphinidin). The 39 core ingredients screened by the ingredient–target network under 3.3 displayed a good binding affinity to the 3CLpro and ACE2 proteins, and their binding energies were <–3.9. The docking results for each core ingredient for 3CLpro and ACE2 are given in Table 4. To further analyze the interaction between the ingredient and the protein, 2D and 3D molecular docking diagrams exhibited the potential interactions between the ingredient and 3CLpro or ACE2. The molecular docking of the ingredients with the best results is shown in Figure 8. Due to the presence of a hydrophobic Pi-alkyl, the 3′-methoxyglabridin parent nucleus was mainly bound to the amino acid residues CYS145, MET165, and PRO168 of 3CLpro. In addition, hydrogen bonds formed between the phenolic hydroxyl groups on the parent nucleus and the amino acid residues GLY143, LEU141, and CYS145. Due to the presence of the hydrophobic Pi-alkyl, the Alisol B 23-acetate parent nucleus bound to the ACE2 amino acid residues LEU85 and HIS15, and the hydroxyl and carbonyl groups on the parent nucleus formed hydrogen bonds with the amino acid residues GLN101 and ASN103. These interactions might increase the binding of the molecules to the proteins.

The Effect of QFPDD on the levels of mRNA transcripts of SRC, MAPK1, PRKCD, PTK2, and PRKCE

In total, 5 out of 24 key target genes with different degree values were selected to verify the effect of QFPDD on inflammation. As shown in Figure 9, compared with the control group, the relative levels of *SRC, MAPK1, PRKCD, PTK2,* and *PRKCE* transcripts increased significantly, which were significantly mitigated in the QFPDD and DXM groups. Of note, the relative levels of *SRC* and *MAPK1* mRNA transcripts in the QFPDD group were slightly higher than those in the DXM group, although they were statistically insignificant.

Discussion

Network pharmacology is based on the systematic interactions between drugs, targets, and diseases and uses complex network models to determine the pharmacological properties of the research

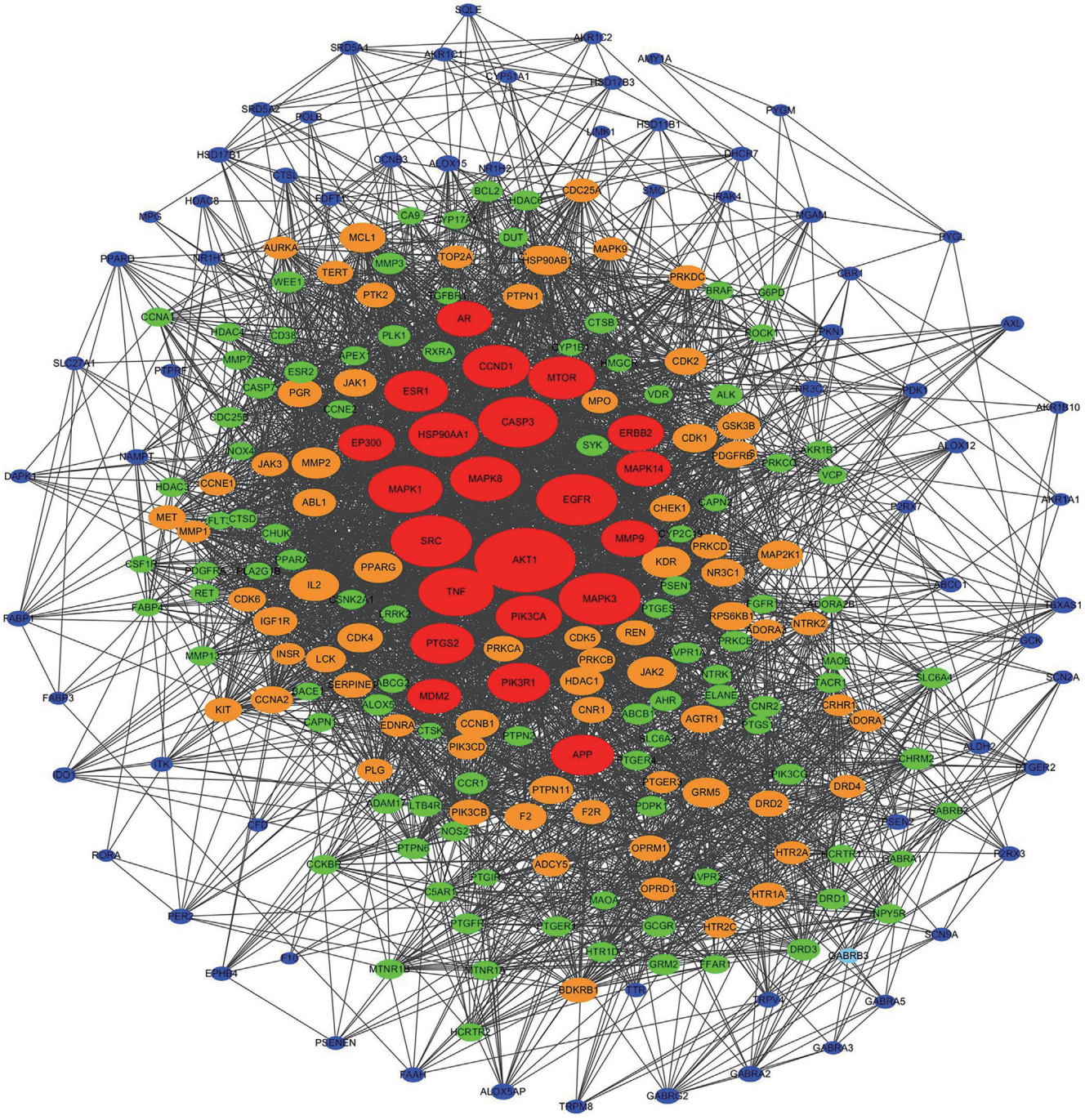

Fig. 5. Genes associated with different signal pathways (the size of the nodes represents the size of the degree). The degree value of the node in this figure reflects the degree of association between genes and disease treatment, and the node in front of the degree value might be a target gene of interest.

objects.[17] The research and development of network pharmacology in TCMs provided a new perspective for the systematic study of the complex ingredients of TCMs.[18–20] Therefore, in this study, the target network for QFPDD and COVID-19 was constructed and analyzed, and the targets were used for functional enrichment and signal pathway analysis to reveal the potential molecular mechanisms that underlie the action of QFPDD for the treatment of COVID-19 and to identify the main active ingredients and potential target genes of QFPDD.

Main active ingredients

Previous studies confirmed that SARS-CoV-2, similar to SARS-CoV, binds to ACE2 and causes infection.[21] Therefore, the ingredient most closely related to the hydrolase and ACE2 of 2019-nCoV

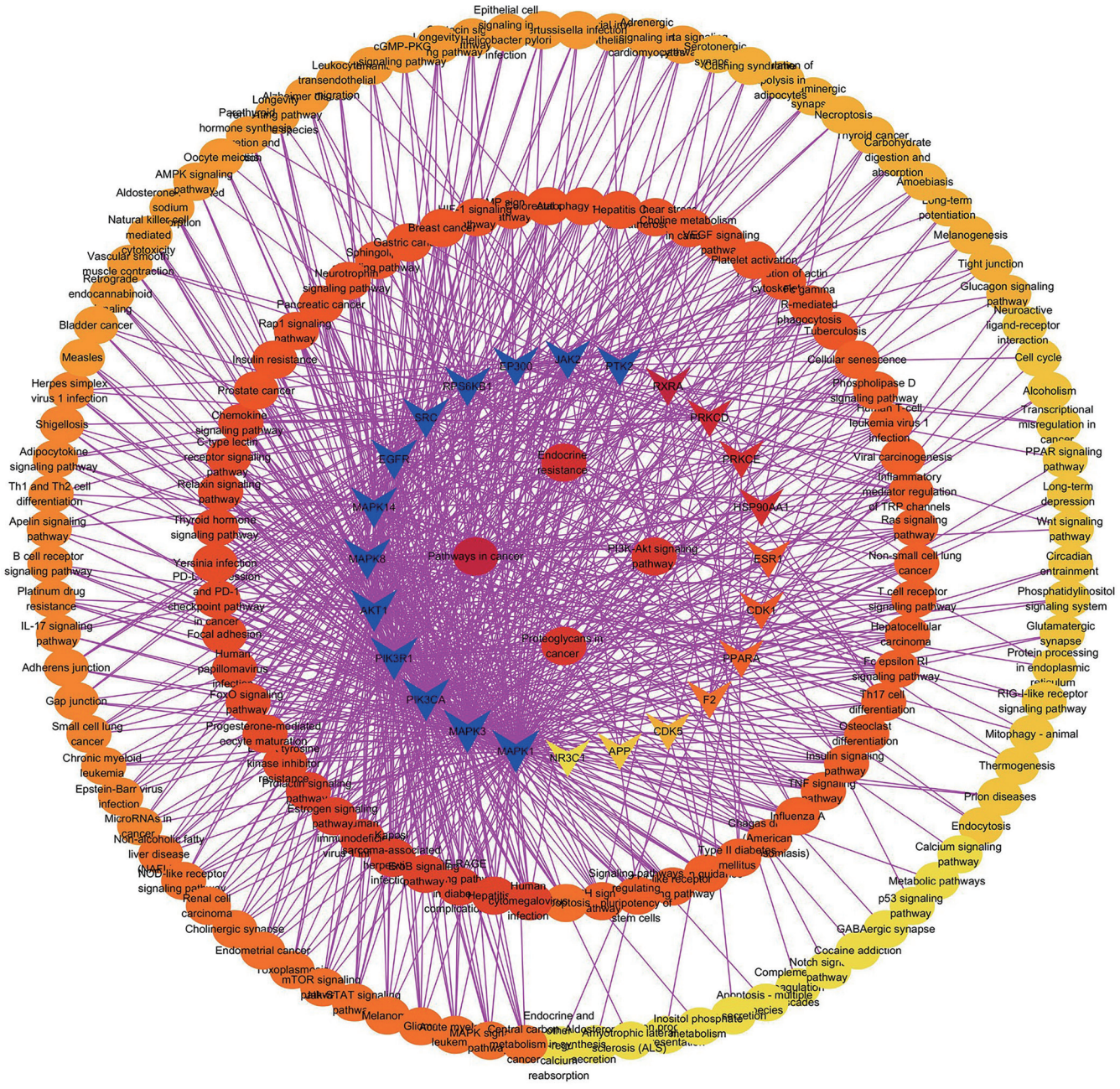

Fig. 6. Target–signal pathway. The circular node represents the signal pathway in which 24 key targets participate, and the v-shaped node represents the 24 key targets. The color of the node represents the ascending order of degree from yellow to orange to red to blue.

3CLpro might be the main bioactive ingredient of QFPDD against SARS-CoV-2-induced COVID-19. This study used 20 TCMs (except for GF) from QFPDD to screen 375 major active ingredients and tested their binding to 3CLpro and ACE2 by molecular docking. The results indicated that except for taraxanthin and delphinidin, the remaining ingredients had binding energies <0 when docking with both proteins, which suggested that these ingredients from QFPDD might bind directly to the proteins, which ameliorated SARS-CoV-2 infection-induced COVID-19. The 39 core ingredients identified through network pharmacology had many targets that might improve disease symptoms and could be closely associated with 3CLpro and ACE2. Therefore, the 39 ingredients might be the main bioactive ingredients for the treatment of COVID-19 by QFPDD.

Potential target genes

This study found 24 key targets (*PIK3CA, PIK3R1, APP, SRC, MAPK1, MAPK3, AKT1, HSP90AA1, EP300, CDK1, JAK2, EGFR, F2, MAPK8, RXRA, ESR1, PRKCD, PTK2, RPS6KB1, MAPK14, NR3C1, PRKCE, CDK5,* and *PPARA*) for the treatment of COV-

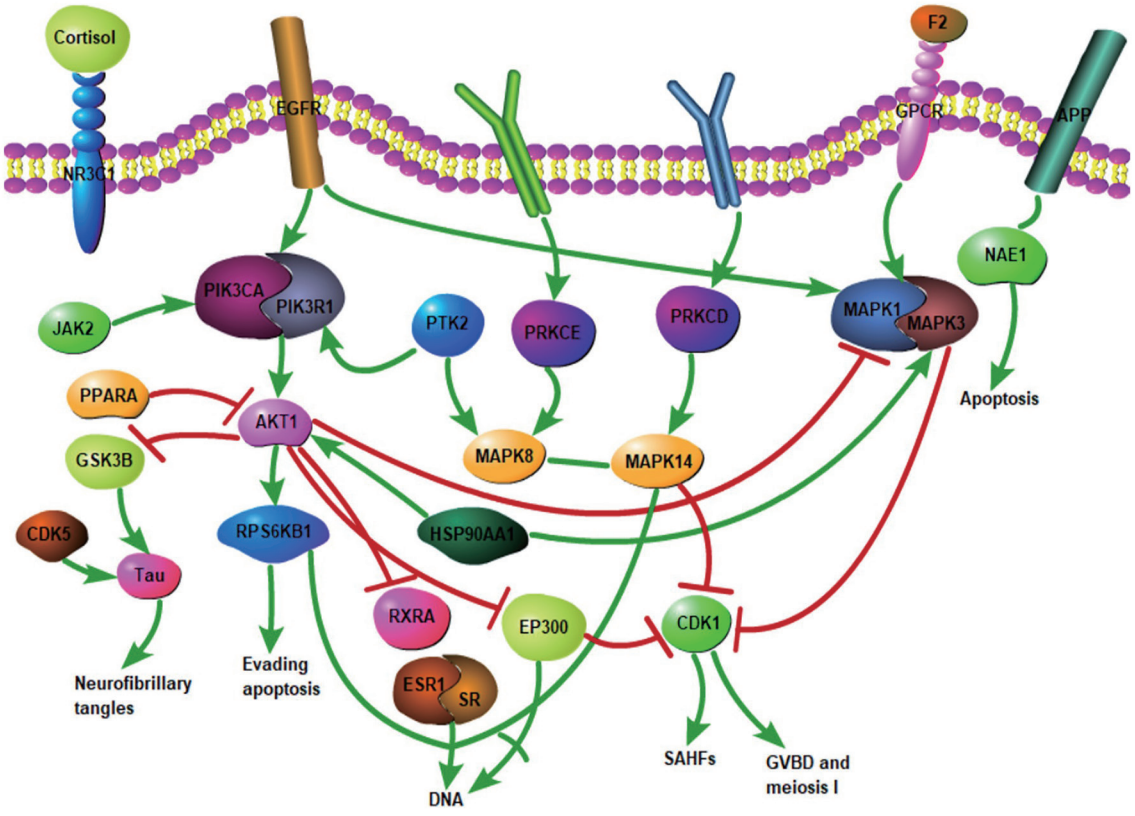

Fig. 7. Twenty-four critical targets for the treatment of COVID-19. All targets are expressed as the gene name.

ID-19. Due to their close association, these targets might interact and act synergistically for the pathogenesis of COVID-19. Aberrant SRC activity contributes to the pathogenesis of pneumonia, which represents a potential target for pneumonia treatment.[22] MAPK activation modulates the inflammatory response in ALI. MAPK1 activation reduces the LPS-induced inflammatory injury in A549 cells and ameliorates lung injury in ALI mice.[23] PRKCD is an important regulator of human neutrophil proinflammatory responses and is crucial to regulate neutrophil–endothelial cell interactions and recruitment in inflamed lungs.[24] The activation of members of the PTK family participate in acute inflammatory responses, during ALI and sepsis, and are essential for the recruitment and activation of monocytes, macrophages, neutrophils, and other immune cells.[25] PRKCE could be used as a breathing regulator by affecting mitochondrial respiration, which promotes the occurrence of mitochondrial organisms and reduces organ damage that is caused by pneumonia.[26] COVID-19 causes severe inflammation and acute lung damage, which leads to severe respiratory distress syndrome. In this study, a cellular model of inflammation was used to verify the relevant targets for QFPDD for inflammation. We found that treatment with QFPDD significantly mitigated the LPS-induced gene expression in A549 cells and that these genes belonged to the 24 potential targets of QFPDD. These findings might help in understanding QFPDD treatment for COVID-19.

Functional enrichment and pathway analysis

The GO functional enrichment analysis revealed the potential targets that were involved in biological processes, molecular function, and cell components.[27] The potential targets of QFPDD were enriched in biological processes that included the cellular response to nitrogen compounds and the positive regulation of transferase activity. A previous study showed that the inhibition of nitric oxide (NO) led to an increase in the release of proinflammatory cytokines, deteriorating lung injury, which suggested that NO might ameliorate ALI.[28] In addition, QFPDD targeted molecules that were mainly associated with protein kinase activity, protein tyrosine kinase activity, and kinase binding. Experimental results have shown that the mitochondrial antioxidant pathway mediated by protein kinase D1 is crucial for the early stage of bleomycin-induced pulmonary fibrosis in rats.[29] Similarly, protein kinase CK2 is related to the prognosis of patients with lung cancer, which suggests that protein kinase CK2 might be a potential target for the treatment of lung cancer.[30] In addition, QFPDD targeted cell components that are mainly associated with the membrane, receptor complex, and dendrite. Experiments demonstrated that the lipid raft protein stomatin, in the presence of low oxygen and Dex upregulation stabilized the cytoskeleton that is connected to the membrane and increased the barrier function of lung epithelial cells, which protected lung tissue cells.[31] The targets by QFPDD might improve the symptoms of COVID-19 patients through the cellular response to nitrogen compounds, protein kinase activity, and membrane rafts. Therefore, the treatment of COVID-19 by QFPDD might be more closely related to these biological processes.

The KEGG pathway analysis exhibited that the enriched pathways were involved in cancer, the neuroactive ligand-receptor interaction, and the PI3K-Akt signal pathway. The 24 predicted key targets of QFPDD were more closely related to the pathways involved in cancer and proteoglycans in cancer, which suggested

Table 4. Docking of the 39 core components with 3CLpro and ACE2

Number	Compound	Binding energy values with 3CLpro (kcal/mol)	Binding energy values with ACE2 (kcal/mol)
1	3′-Methoxyglabridin	−8.3	−6.1
2	Moslosooflavone	−7.8	−6.0
3	Kaempferol	−7.7	−5.9
4	Alisol,b,23-acetate	−7.7	−6.8
5	Quercetin	−7.6	−6.2
6	Peroxyergosterol	−7.6	−5.8
7	Diosmetin	−7.6	−6.3
8	Genkwanin	−7.6	−5.9
9	Epianhydrobelachinal	−7.6	−6.5
10	α-Amyrin	−7.5	−6.7
11	[(1S,3R)-1-[(2R)-3,3-dimethyloxiran-2-yl]-3-[(5R,8S,9S,10S,11S,14R)-11-hydroxy-4,4,8,10,14-pentamethyl-3-oxo-1,2,5,6,7,9,11,12,15,16-decahydrocyclopenta[a]phenanthren-17-yl]butyl] acetate	−7.5	−6.8
12	Areapillin	−7.4	−6.3
13	Naringenin	−7.3	−5.9
14	Glyasperin B	−7.3	−5.7
15	5,8,2′-Trihydroxy-7-methoxyflavone	−7.2	−6.1
16	Galangin	−7.2	−6.0
17	Spinasterol	−7.1	−5.6
18	Cerevisterol	−7.1	−5.6
19	3beta-Hydroxy-24-methylene-8-lanostene-21-oic acid	−7.0	−6.3
20	Poriferast-5-en-3beta-ol	−7.0	−5.5
21	Stigmasterol	−7.0	−5.5
22	beta-sitosterol	−6.9	−6.8
23	Sinensetin	−6.9	−5.5
24	Dehydroeburicoic acid	−6.8	−5.8
25	Alisol B monoacetate	−6.8	−6.0
26	(22e,24r)-ergosta-6-en-3beta,5alpha,6beta-triol	−6.8	−5.5
27	Glypallichalcone	−6.7	−5.4
28	Femara	−6.7	−5.3
29	5,7-dihydroxy-2-(3-hydroxy-4-methoxyphenyl)chroman-4-one	−6.6	−5.5
30	Trametenolic acid	−6.6	−6.4
31	3,5,6,7-tetramethoxy-2-(3,4,5-trimethoxyphenyl)chromone	−6.5	−5.4
32	Sitosterol	−6.5	−5.7
33	Tussilagolactone	−6.5	−4.8
34	Denudatin B	−6.5	−5.4
35	Anhydrobelachinal	−6.5	−5.8
36	(3S,8S,9S,10R,13R,14S,17R)-10,13-dimethyl-17-[(2R,5S)-5-propan-2-yloctan-2-yl]-2,3,4,7,8,9,11,12,14,15,16,17-dodecahydro-1H-cyclopenta[a]phenanthren-3-ol	−6.4	−5.0
37	4,9-dimethoxy-1-vinyl-$b-carboline	−6.3	−5.7
38	Kadsurenone	−6.1	−5.2
39	Gondoic acid	−4.7	−3.9

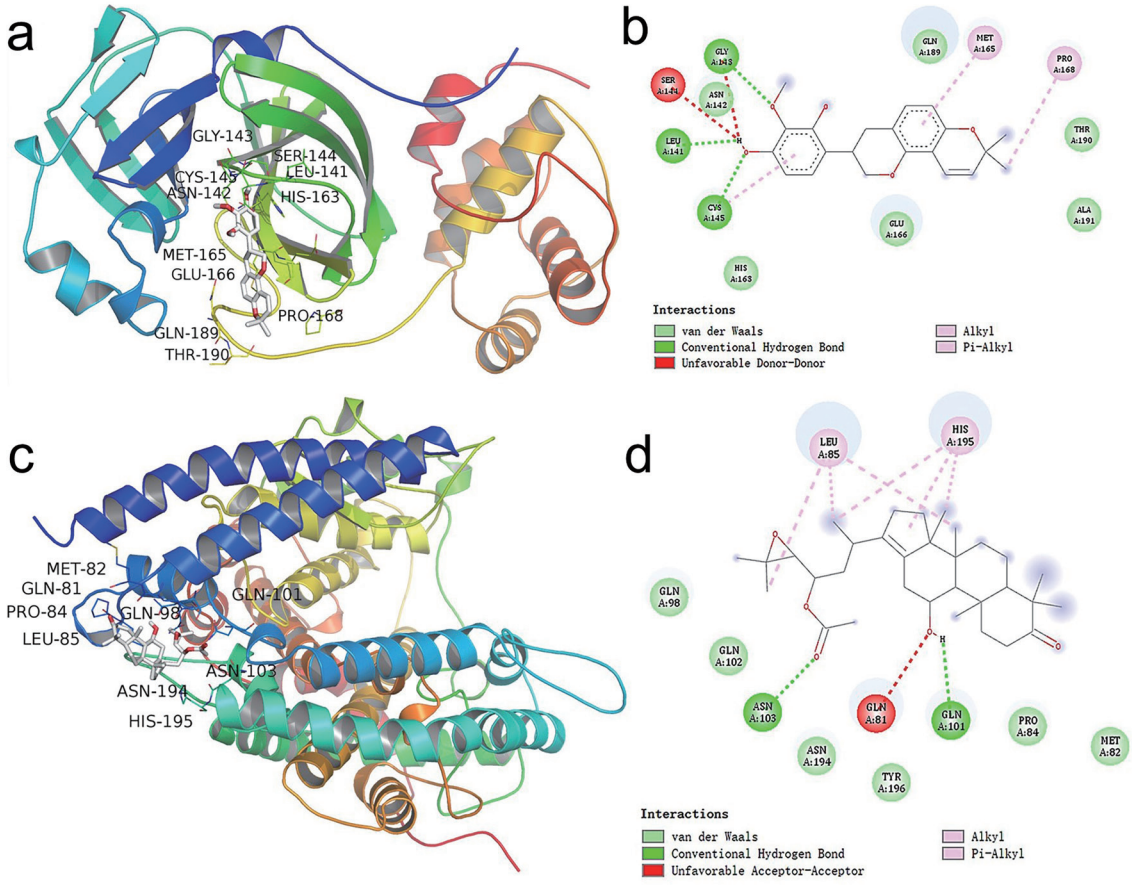

Fig. 8. 2D and 3D diagrams of the molecular docking of: (a and b) 3CLpro with 3′-methoxyglabridin; and (c and d) ACE2 with Alisol B 23-acetate.

that the pathogenesis of COVID-19 might have similar processes to cancer. A recent study demonstrated that the risk of COVID-19 infection in cancer patients was 2.31-fold higher than that of the general population in Wuhan.[32] Cancer patients might have a low immune function, which could promote virus infection, or have a poor function in the key target genes, or both. Most of the 24 potential targets of QFPDD were closely related to cancer development.[33] carcinogenic signal pathways, which included the PI3K-Akt-mTOR, MAPK-ERK, SRC, CDK4-CDK6, and ER pathways, which are critical for endocrine resistance. Targeting these pathways, especially the ER pathway, could be the most effective way to combat resistance to anti-estrogens, and clinical trials have shown promising results. The PI3K-Akt signal pathway regulates the cellular inflammatory response by stimulating the expression of endothelial nitric oxide synthase (eNOS) and increasing the production of NO to increase vascular permeability, promote the infiltration of inflammatory cells, stimulate the activation of inflammatory cells, and induce the secretion of a large number of inflammatory factors through the activity of NO.[34] Studies demonstrated that PI3K inhibitors had a significant inhibitory effect on NO production and inflammatory response in lung tissues of a viral pneumonia mouse model induced by influenza A virus infection.[35] In addition to TCMs for COVID-19, some anti-virus (HIV or Ebola) drugs inhibit SARS-CoV-2 replication to ameliorate COVID-19 in the clinic. In this study, we found that 24 genes participated in the signal pathways associated with human immunodeficiency virus infection, which might explain why remdesivir and lopinavir or ritonavir have some benefits to COVID-19 patients.

Future directions

QFPDD is characterized by multiple components, multiple targets, and multiple pathways to treat COVID-19, which could improve the clinical symptoms of patients. The 39 active components, 24 potential key targets, and signaling pathways, such as the PI3K-Akt signaling pathway in QFPDD we found could provide a basis for further study of QFPDD and provide a reference for the development of new drugs for the treatment of COVID-19. In the future, the 39 active ingredients and related signaling pathways should be verified to clarify the material basis and other pharmacological effects of QFPDD for the treatment of COVID-19, such as organ protection, enhancement of immunity, and other functions.

Conclusions

In this study, 39 active ingredients from QFPDD were involved in the treatment of COVID-19 through a network pharmacology analysis, and 24 potential target genes for QFPDD were identified. These were involved in several biological processes and signal pathways, because some ingredients are directly bound to ACE2 and 3CLpro and these targets might be valuable for the treatment

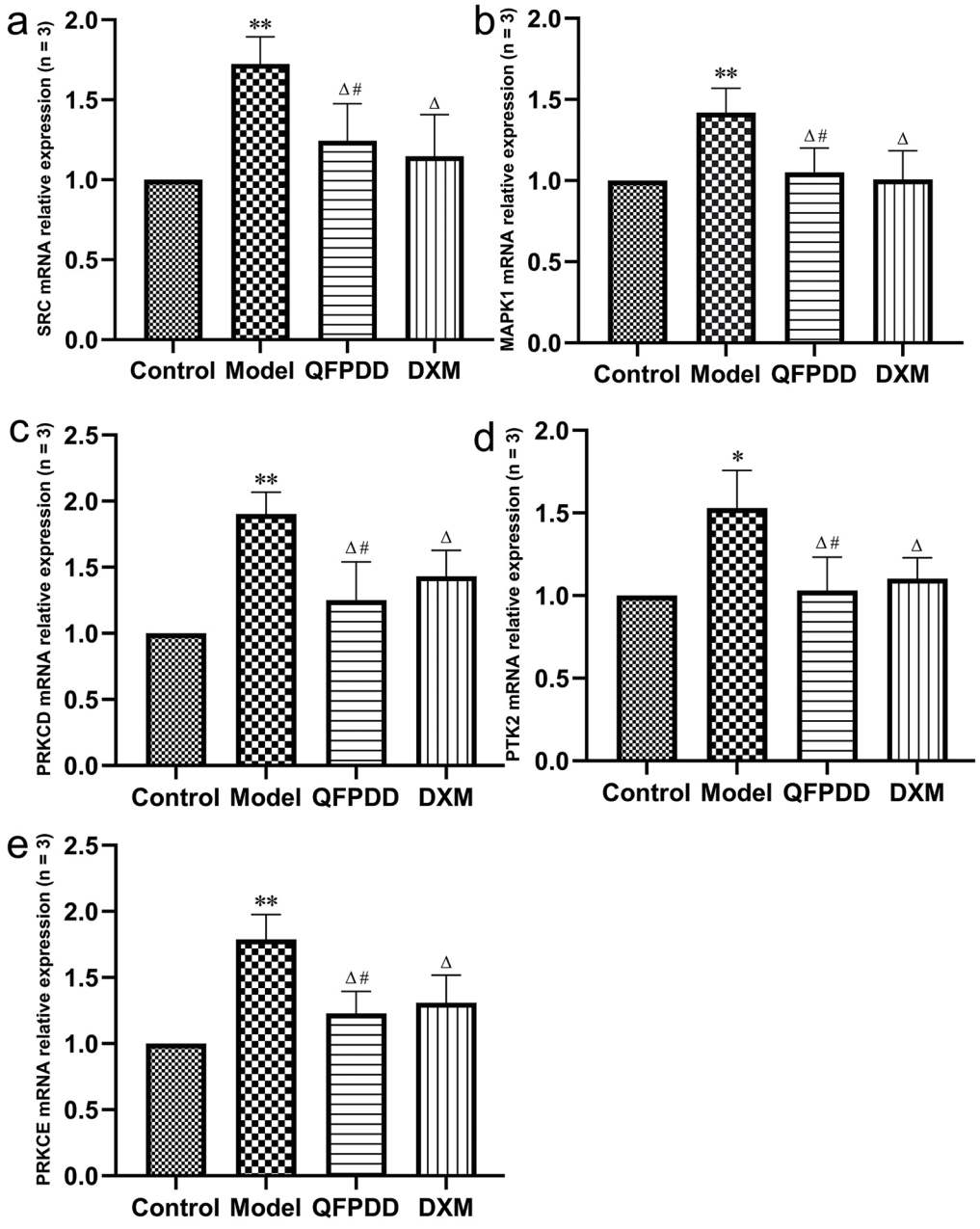

Fig. 9. RT-qPCR analysis of the relative levels of *SRC, MAPK1, PRKCD, PTK2,* and *PRKCE* mRNA transcripts. A549 cells were stimulated with or without (control), LPS alone (model) or LPS together with QFPDD or dethamemasone for 24 h and the relative levels of each gene mRNA transcripts were quantified by RT-qPCR. The levels of each gene mRNA transcripts in the control group were designated as 1: (a) levels of SRC mRNA transcripts; (b) levels of MAPK1 mRNA transcripts; (c) levels of PRKCD mRNA transcripts; (d) levels of PTK2 mRNA transcripts; and (e) levels of PRKCE mRNA transcripts $^{**}p<0.01$ or $^{*}p<0.05$ compared with the control group; $^{\Delta}p<0.05$ compared with the model group, $^{\#}p>0.05$ compared with the DXM group.

of COVID-19. The active ingredients of QFPDD may synergistically target multiple targets to improve clinical symptoms in COVID-19 patients. The 24 potential target genes were primarily involved in inflammatory responses during the pathogenic process of COVID-19 by participating in pathways that are associated with cancer, endocrine resistance, PI3K-Akt signaling, and proteoglycans. Therefore, our findings might provide a foundation for further exploration of QFPDD for the treatment of COVID-19. Further studies are required to verify the material basis-pharmacodynamic evaluation-metabolomics-signaling pathway network to provide an experimental basis for the treatment of COVID-19 with QFPDD and further drug development.

Supporting information

Supplementary material for this article is available at https://doi.org/10.14218/JERP.2021.00011.

Supplementary Document 1. Twenty TCMs' ingredients or abbreviations and the targets of the major COVID-19 clinical symptoms.

Supplementary Document 2. The targets of 20 TCMs' active ingredients in QFPDD.

Acknowledgments

None.

Funding

This work was supported by the key research and development project of Shandong province: demonstration research on key technologies of precision and industrialization of TCM prescription (2016CYJS08A01)

Conflict of interest

The authors declare that they have no conflict of interest.

Author contributions

Study concept and design, analysis and interpretation of data, prepared figures, wrote the manuscript text (YL, LWX); acquisition of data (YYW, MXL); critical revision of the manuscript for important intellectual content, obtained funding (LFZ, YQZ); All authors reviewed the manuscript.

Data availability

The datasets used or analyzed during the present study are available from the corresponding author upon reasonable request.

References

[1] Ji JS. Origins of MERS-CoV, and lessons for 2019-nCoV. Lancet Planet Health 2020;4(3):e93. doi:10.1016/S2542-5196(20)30032-2.
[2] Zhang L, Zheng X, Bai X, Wang Q, Chen B, Wang H, *et al*. Association between use of Qingfei Paidu Tang and mortality in hospitalized patients with COVID-19: A national retrospective registry study. Phytomedicine 2021;85:153531. doi:10.1016/j.phymed.2021.153531.
[3] Hopkins AL. Network pharmacology: the next paradigm in drug discovery. Nat Chem Biol 2008;4(11):682–690. doi:10.1038/nchembio.118.
[4] Li ZP, Chen HJ, Chang SH, Lou Y, Han ZM. Variation of Th17/Treg cell balance and Notch signaling pathway in children with mycoplasmal pneumonia (in Chinese). Chinese Journal of Nosocomiology 2020; 30(7):1048–1052.
[5] Duan RQ, Li CQ. Effects of azithromycin and montelukast sodium on NOD-like receptor protein-3 inflammatory pathway in children with mycoplasma pneumonia (in Chinese). China Medical Engineering 2019; 12:90–92.
[6] Tan H, Ji H, Li N, Zhang XJ, Jia Y. Relationship between TGF-β and ERK/GSK3β activation of signaling pathway and radiation-induced mesenchymal transformation of alveolar epithelial cells in rats with radiation-induced pneumonia (in Chinese). Journal of Guangxi Medical University 2019;36(12):1909–1914. doi:10.16190/j.cnki.45-1211/r.2019.12.007.
[7] Xue JJ, Shi XX. Expression of TLRs in peripheral blood mononuclear cells of children with mycoplasma pneumonia and its effect on NF-κB/IκBα pathway. Chinese Journal of Health Laboratory Technology 2019;29(20):11–14.
[8] Wang TT, Leng CH, Guo KP, Jin SJ. Effect of quercetin on the prevention and treatment of staphylococcus aureus pneumonia in mice and the mechanism of IKK/NF-κB/IκB signaling pathway (in Chinese). Pharmacology and Clinics of Chinese Materia Medica 2019;35(4):53–57.
[9] Wang XK. Experimental study on prevention and treatment of radioactive pneumonia by regulating AMPK mediated autophagy by qingfei yiyin prescription [Dissertation] (in Chinese). Beijing: China Academy of Traditional Chinese Medicine; 2019.
[10] Liu ZM, Sun Y, Gao YC, Long HC, Lei T, Du HJ. Effects of Nomilin on inflammatory response in Klebsiella-induced geriatric pneumonia rats (in Chinese). Chinese Journal of Immunology 2019;35(8):970–975. doi:10.3969/j.issn.1000-484X.2019.08.016.
[11] Huang P, Guo YH, Xu XL, He SS, Liu QQ. The role of PI3K/Akt/mTOR signaling pathway in the regulation of Treg/Th17 balance in severe pneumonia and the research progress of traditional Chinese medicine (in Chinese). Journal of Emergency in Traditional Chinese Medicine 2018;27(12):183–185.
[12] Huang YX. Effect of rhIFN-α1b on RSV infection in rats and the signaling pathways of JAK/STAT and TLR4/NF-κB [Dissertation] (in Chinese). Xi'an: The Fourth Military Medical University; 2015.
[13] Hui GM. Effect of qingfei peiyuan granule on IL-17 and JAK-STAT signaling pathways in BALB/c mouse model of immunocompromised lung infection [Dissertation] (in Chinese). Henan: Henan University of Traditional Chinese Medicine; 2014.
[14] Mei X. Effects of toxin clearance on JAK/STAT signal transduction pathway in lung tissue of rats with phlegm-heat syndrome of pneumonia [Dissertation] (in Chinese). Henan: Henan University of Traditional Chinese Medicine; 2010.
[15] Guo XK. Study on the role of HIF-1α in the regulation of inflammatory factors by nuclear translocation in severe pneumonia caused by influenza a (H1N1) virus infection [Dissertation] (in Chinese). Shanghai: Shanghai Jiao Tong University; 2017.
[16] Wang XF, Chen SY, Chen F. Progress in role of Epac/Rap1 signal pathway in acute lung injury (in Chinese). Chinese Journal of Pharmacology and Toxicology 2012;26(5):680–683. doi:10.3867/j.issn.1000-3002.2012.05.015.
[17] Zhou WX, Cheng XR, Zhang YX. Network pharmacology: a new concept of drug discovery and understanding (in Chinese). Chinese Journal of Pharmacology and Toxicology 2012;26(1):4–9.
[18] Zhang WJ, Wang YH. Principle and method of systematic pharmacology and it's application in traditional Chinese medicine. World Chinese Medicine 2015;10(2):280–286.
[19] Zhang YQ, Li S. dvances in network pharmacology and modern research of traditional Chinese medicine (in Chinese). Chinese Journal of Pharmacology and Toxicology 2015;29:883–892.
[20] Wang YH, Yang L. Systems Pharmacology-Based Research Framework of Traditional Chinese Medicine (in Chinese). World Chinese Medicine 2013;8(7):801–808.
[21] Zhou P, Yang XL, Wang XG, Hu B, Zhang L, Zhang W, *et al*. A pneumonia outbreak associated with a new coronavirus of probable bat origin. Nature 2020;579(7798):270–273. doi:10.1038/s41586-020-2012-7.
[22] Lee D, Gautschi O. Clinical development of SRC tyrosine kinase inhibitors in lung cancer. Clin Lung Cancer 2006;7(6):381–384. doi:10.3816/clc.2006.n.020.
[23] Zhu S, Song W, Sun Y, Zhou Y, Kong F. MiR-342 attenuates lipopolysaccharide-induced acute lung injury via inhibiting MAPK1 expression. Clin Exp Pharmacol Physiol 2020;47(8):1448–1454. doi:10.1111/1440-1681.13315.
[24] Mondrinos MJ, Zhang T, Sun S, Kennedy PA, King DJ, Wolfson MR, *et al*. Pulmonary endothelial protein kinase C-delta (PKCδ) regulates neutrophil migration in acute lung inflammation. Am J Pathol 2014;184(1):200–213. doi:10.1016/j.ajpath.2013.09.010.
[25] Okutani D. Src protein tyrosine kinase family and acute lung injury (in Japanese). Nihon Rinsho Meneki Gakkai Kaishi 2006;29(5):334–341. doi:10.2177/jsci.29.334.
[26] Aslami H, Pulskens WP, Kuipers MT, Bos AP, van Kuilenburg AB, Wanders RJ, *et al*. Hydrogen sulfide donor NaHS reduces organ injury in a

rat model of pneumococcal pneumosepsis, associated with improved bio-energetic status. PLoS One 2013;8(5):e63497. doi:10.1371/journal.pone.0063497.
[27] Wang X, Yin TS, Li BY, Jiang XL, Sun H, Dou YG, *et al*. Progress of gene function enrichment analysis (in Chinese). Chinese Science: Life Science 2016;46(4):363–373.
[28] Qiu HB, Chen DC, Pan JQ. Regulatory effect of inhibition of nitric oxide synthesis on inflammatory response in acute lung injury (in Chinese). Chinese Journal of Emergency Medicine 1999;8(3):153–155. doi:10.3760/j.issn:1671-0282.1999.03.004.
[29] Ni N. Effect of active vitamin D3 on d1-mediated antioxidant pathway in rat pulmonary fibrosis (in Chinese). Chinese Journal of Anatomy 2016;39:534–538.
[30] Li QW. Inhibition of protein kinase CK2 activity enhances radiosensitivity of non-small cell lung cancer and its mechanism [Dissertation] (in Chinese). Hubei: Huazhong University of Science and Technology; 2018.
[31] Lu J, Chen JC, Cai HY, Ma YY, Wang Y. Expression of lipidin stomatin in rat lung and A549 cells induced by hypoxia or/and glucocorticoid and its effect on cytoskeleton (in Chinese). Chinese Journal of Pathophysiology 2010;10:2072–2072.
[32] Yu J, Ouyang W, Chua MLK, Xie C. SARS-CoV-2 Transmission in Patients With Cancer at a Tertiary Care Hospital in Wuhan, China. JAMA Oncol 2020;6(7):1108–1110. doi:10.1001/jamaoncol.2020.0980.
[33] Miller TW. Endocrine resistance: what do we know? Am Soc Clin Oncol Educ Book 2013;33:e37–e42. doi:10.1200/EdBook_AM.2013.33.e37.
[34] Yin XL, Zhang JY, Liu WD, Duo Jiu HY, Cui H. Sphingosine 1-phosphate receptor 2 mediates PI3K/AKT/eNOS pathway to inhibit viral pneumonia induced by influenza A virus (in Chinese). Chinese Journal of Pathophysiology 2008;34(11):150–155.
[35] Yang YL, Tu ML, Xie MS. Effects of PI3K inhibitor on NO production and inflammatory response in lung tissues of viral pneumonia mice induced by influenza a virus FM1 infection (in Chinese). Chinese Journal of Virology 2019;35(5):713–720. doi:10.13242/j.cnki.bingduxuebao.003597.